# Photochromic Liquid Crystalline Cyclic Siloxanes Containing Spiropyran Groups

**L. V. Natarajan,*,† T. J. Bunning,‡ and S. Y. Kim§**

*Science Applications International Corporation, 101 Woodman Drive, Dayton, Ohio 45431, Materials Directorate, Wright Laboratory, Wright Patterson Air Force Base, Ohio 45433, and Chemistry Department, Wright State University, Dayton, Ohio 45432*

*Received May 29, 1994; Revised Manuscript Received July 18, 1994®*

ABSTRACT: The effects of covalently incorporating a T-shaped photochromic spiropyran molecule with cholesterol- and biphenyl-substituted mesogens to a cyclic siloxane backbone on the liquid crystalline behavior of the resulting macromolecular siloxanes are reported. The siloxanes containing up to 20% spiropyran are liquid crystalline, whereas at higher compositions the products are amorphous. With increasing spiropyran content, the selective reflection band characteristic of the cholesteric mesophase shifted to lower wavelengths. The photochromic reaction leading to the blue merocyanine formation resulted in a narrowing of the reflection bandwidth. Steric effects imposed by cholesterol, biphenyl, and bulky spiropyran groups dominate the thermal decoloration kinetics of the merocyanine form. Aggregation of merocyanines was observed in nonpolar solvents, whereas in thin glassy films formed by shearing in the liquid crystalline state such an observation was not evident. In siloxanes bound only to spiropyran, an evidence of a shift in the thermal equilibrium toward merocyanine aggregate formation leading to molecular stacks was observed. Short spacer length of the leader group in spiropyran inhibited 100% attachment to the cyclic siloxane backbone, possibly due to steric effects. Longer spacer groups facilitated 100% attachment.

## Introduction

In recent years, there has been a growing interest in polymers containing siloxane groups. Siloxane polymers are materials of significant technological interest. The unique physical and chemical properties of the siloxane polymers may be attributed to the siloxane bond (Si–O) which offers a highly flexible structural unit yielding polymer chains with low glass transitions ($T_g$) and surface tensions.[1] Attachment of rodlike mesogens to linear and cyclic siloxane rings enhanced the $T_g$'s and resulted in liquid crystalline (LC) polymers possessing anisotropic properties. Binding cholesterol and biphenyl mesogens to cyclic siloxane backbones gave rise to cholesteric siloxanes capable of forming clear glasses by shear casting from the mesophase.[2] By quenching the aligned cholesteric phase to a glass by cooling to room temperature, films exhibiting selective reflection from the UV to the near-IR was observed. Interestingly, birefringent fibers can be drawn from the melt of these low molecular weight siloxanes. Covalently linking azo dyes to these siloxanes led to potential reversible optical data storage materials.[3] Incorporating nonlinear chromophores in this structure resulted in materials capable of second harmonic generation.[4]

Developing materials exhibiting both liquid crystallinity and photochromism is indeed a challenging task. Often, such attempts result in loss of one or both of these properties. Spiropyrans are well-known organic molecules with photochromic, thermochromic, and solvatochromic properties. They undergo conversion to colored merocyanine dyes in the presence of light, upon heating, or by dissolving in highly polar solvents.[5] This reaction is reversible by irradiation with light or heat (Figure 1a). By carefully designing synthetic routes, Krongauz

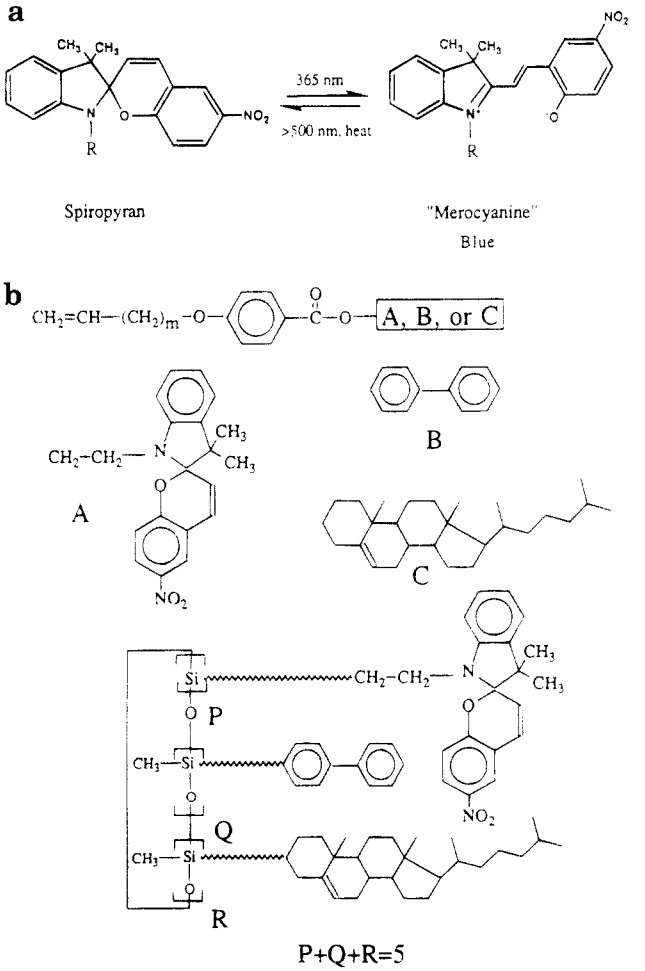


**Figure 1.** (a) Photochromism of 6-nitrospiropyran. (b) Structure of cyclic siloxane bonded to the mesogens.

and co-workers demonstrated photochromic properties in a number of liquid crystalline and polymeric liquid crystalline systems containing spiropyran or spirooxazines.[5–9] Krongauz et al.[9] found that photochromic spironaphthoxazine side groups incorporated

* Author to whom correspondence should be addressed.
† Science Applications International Corp.
‡ Wright Patterson Air Force Base.
§ Wright State University.
® Abstract published in *Advance ACS Abstracts,* October 15, 1994.

0024-9297/94/2227-7248$04.50/0 

in liquid crystalline poly(siloxane) with (*p*-cyanophenyl)-benzoate side groups had glass transition temperatures below room temperature. The fast thermal decoloration observed was attributed to the lack of aggregation of the merocyanine form. Steric effects inhibited the 100% attachment of the spironaphthoxazines containing short spacers to cyclic siloxanes.[10]

We recently reported preliminary results on the synthesis of a liquid crystalline cyclic siloxane made up of photochromic spiropyran, biphenyl, and cholesterol moieties.[11,12] This siloxane, when melted and shear cast, formed a cholesteric film exhibiting selective reflection. These films were used to write, erase, and rewrite holograms.[13] Writing was achieved by UV laser light (358 nm) which led to opening of the closed spiropyran to the blue merocyanine form, and heating the film to 60 °C led to the disappearance of the blue due to the formation of the closed form (Figure 1a). In this paper, we report on the synthesis, characterization, and photochromic behavior of a number of cyclic siloxanes containing biphenyl, cholesterol, and spiropyran (Figure 1b). The influences of a lateral attachment of the photochromic spiropyran molecule on the packing behavior of the biphenyl, cholesterol mesogens around the cyclic siloxane ring and the changes in the phase behavior with varying compositions of the mesogens are discussed. We have also examined the photochromic behavior of the siloxane-bound spiropyran. We have also attempted 100% attachment of the spiropyran mesogen to the siloxane ring by lengthening the spacer group on the spiropyran moiety.

## Experimental Procedures

**Materials.** The following chemicals were used without further purification from Aldrich: 4-hydroxybenzoic acid, potassium hydroxide, allyl bromide, and 5-bromo-1-pentene. (1′-β-Hydroxyethyl)-6-nitro-3,3′-dimethylspiro(2*H*-1-benzopyran-2,2′-indoline) (BIPS) from Chroma Chemicals was used as received. Pentamethylhydrocyclopentasiloxane was obtained from Huls America and vacuum-distilled before use.

**Synthesis.** (Allyloxy)benzoic acid and (pentenyloxy)benzoic acid were synthesized as previously reported.[11] Esterification of these compounds onto cholesterol, hydroxybiphenyl, or BIPS was performed with *N,N′*-dicyclohexylcarbodiimide and (dimethylamino)pyridine using a previously reported method.[14] The products, (allyloxy)benzoate 6-nitrobenzospiropyran (AlBIPS) and (pentenyloxy)benzoate 6-nitrospiropyran (PtBIPS), were purified by repeated crystallization from appropriate solvents and column chromatography. The structure of all the mesogens were confirmed by elemental analysis, FTIR, and $^1$H-NMR. Attachment to the cyclic methylsiloxanes (Huls America) shown in Figure 1b was performed using standard hydrosilation chemistry with a dicyclopentadienylplatinum-(II) chloride catalyst. The platinum catalyst was synthesized per the method of Drew.[15]

Hydrosilation reactions were carried out in toluene at 80–90 °C under argon. Reaction progress was followed by monitoring the disappearance of the Si–H stretch at 2155 cm$^{-1}$ using FTIR spectroscopy. Upon completion, the reaction solution was filtered into methanol to precipitate the product. This was done repeatedly until TLC showed no residual alkene remained in the product. $^1$H-NMR was used to examine the composition of each pendant group on the backbone.

**Characterization Techniques.** Thermal analysis was done on a Perkin-Elmer DSC-2C instrument at 10 °C/min. Second heating and cooling curves were used. A Nikon Optiphot-Pol microscope, Mettler FP82HT hot-stage, and Mettler FP90 Central Processor were used to perform polarized optical light microscopy (POM). $^1$H-NMR was done on a Bruker AM-360 spectrometer. Progress of the hydrosilation reactions was monitored on a Perkin-Elmer 1725X FTIR instrument. The reflection properties of melted thin films cast between glass slides were measured with a Perkin-Elmer Lambda 4B UV–vis spectrophotometer equipped with an integrating sphere. Optical absorption and thermal decoloration kinetic measurements were made with a Perkin-Elmer Lambda 9 spectrophotometer. A fast scan speed of 960 nm/min was used to scan the spectrum in toluene. Fluorescence measurements were made with a Perkin-Elmer LS-50 fluorometer. X-ray diffraction was performed using a Rigaku RU-300 rotating anode diffractometer employing a Statton camera with sample to film distances of 50, 72.9, and 170 mm. Graphite monochromated Cu Kα radiation was utilized with exposure times ranging from 2–24 h. Samples in the form of either thin films heated between Teflon at the desired temperature followed by quenching or packed quartz capillary tubes annealed in the mesophase were examined.

**Table 1. Compositions of Hydrosilation Products as Determined by $^1$H-NMR of the Siloxanes[a]**

| compd | leader on A | A/B/C ratio theoretical | A/B/C ratio estimated |
|---|---|---|---|
| **I** | a | 0/50/50 | 0/50/50 |
| **II** | a | 10/45/45 | 4.6/47.7/47.7 |
| **III** | a | 15/42.5/42.5 | 10.5/44.7/44.7 |
| **IV** | a | 20/40/40 | 15/42.5/42.5 |
| **V** | a | 50/25/25 | 45/27.5/27.5 |
| **VI** | a | 100/0/0 | 75/0/0 |
| **VII** | b | 100/0/0 | 100/0/0 |
| **VIII** | a | 10/90/0 | 8.7/91.3/0 |
| **IX** | a | 10/0/90 | 7.9/0/92.1 |

[a] The mesogens A, B, and C are shown in Figure 1. "a" refers to allyloxy leader; "b" refers to pentenyloxy leader group.

## Results and Discussion

**Addition of Spiropyran to Cyclic Siloxane.** Table 1 shows the final compositions as determined by $^1$H-NMR for all nine compounds. Compound **I** without spiropyran, containing equal amounts of cholesterol and biphenyl, is listed for comparison purposes. The aromatic peaks from the benzoate of the biphenyl and cholesterol molecules at 8.0 and 8.1 ppm and the allylic resonance at 4.6 ppm from the spiropyran molecule were used to calculate compositions using integral areas. In all cases, no residual alkene remained as determined by both TLC and NMR. A small amount of propene elimination (5%) was observed for the allyloxy spacer compounds as reported previously.[16]

In all cases, the observed composition of spiropyran in siloxanes was less than the expected value. This difference is attributed to steric hindrance due to the T-shaped spiropyran core (Figure 1b) when attaching in the presence of other large mesogens. As the sum total of cholesterol and biphenyl increased, the difference between the expected and measured amount of spiropyran also increased. **II** exhibited 46% of the expected amount of spiropyran (4.6/10), while **V** exhibited 90% (45/50). Although no difference in terminal vinyl reactivity is expected among the three mesogens, the rod-shaped cholesterol and biphenyl mesogens can pack more efficiently than the bulky T-shaped spiropyran molecule. There seems to be an upper limit for the amount of spiropyran that could be attached to the siloxane ring, irrespective of the spiropyran content in the reaction mixture. In **VI** having a three-carbon spacer, only 73% ($^1$H-NMR) of the available reactive sites (Si–H) were modified indicating a steric barrier these T-shaped molecules cannot overcome. Attachment with a longer five-carbon spacer group in **VII** did however result in a 100% attachment of the spiropyran molecules. The increased flexibility of this spacer group allows the steric barrier to be overcome.

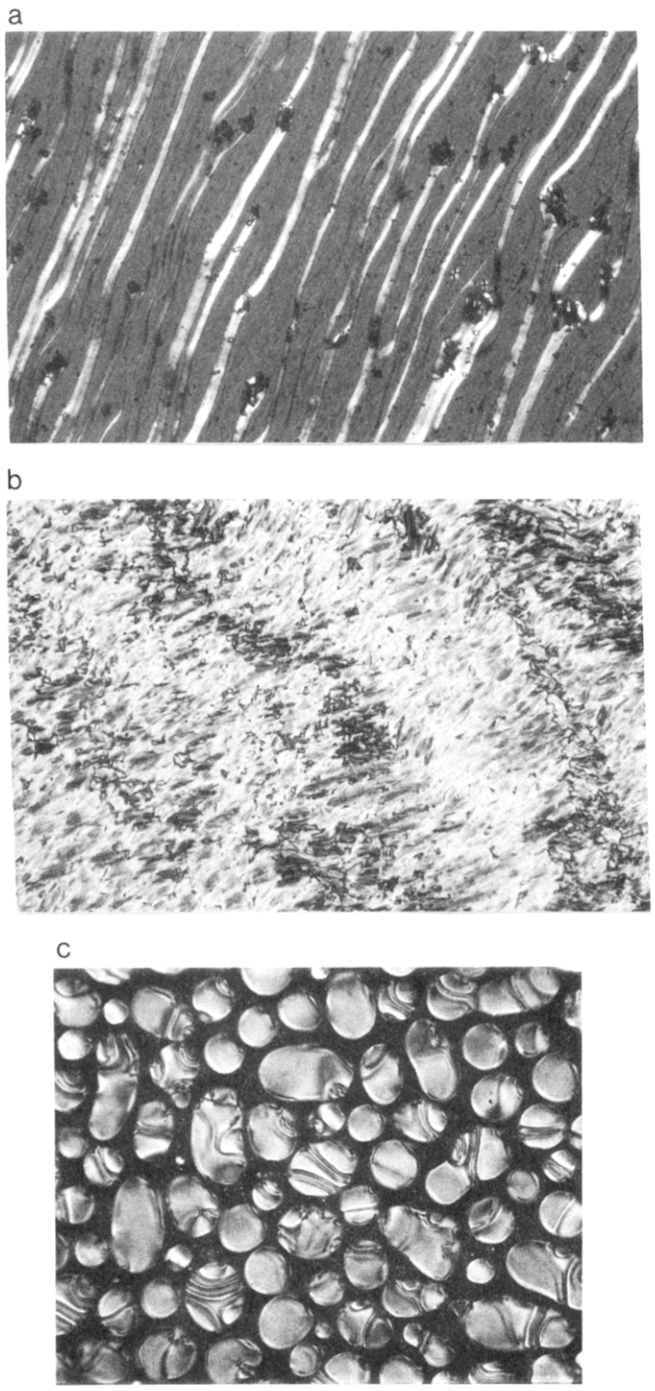


**Figure 2.** (a) POM picture of compound **IX** showing Grandjean oily streaks characteristic of cholesteric phase. (b) POM picture of compound **IX** showing a lower temperature focal-conic fans and homeotropic regions typical of a smectic-A phase. (c) POM picture of large nematic droplets of compound **VIII**.

The progress of the hydrosilation reaction, monitored from the Si−H stretch (2155 $cm^{-1}$) intensity, was also affected by spacer group length and composition. **I**−**V**, **VIII**, and **IX** (Table 1) went to completion within 24 h as indicated by FTIR. **VI** did not proceed after 73% substitution in 45 h, after which time the Si−H stretch did not decrease in intensity. **VII** went to 100% completion in 23 h, indicating that lengthening of the distance between the reactive vinyl bond and the T-shaped mesogen increases its ability to react. Similar behavior was also observed by Krongauz.[10] Krongauz showed that no dependence on the reaction rate was observed when the starting ratio of spirooxazine to the siloxane backbone was low but a large dependence was observed when percentages approached 100. The propene-substituted spirooxazine reacted slower than the hexene-substituted photochrome.[10]

**Phase Behavior.** The thermal transitions and the selective reflection data for all the compounds are shown in Table 2. With increasing spiropyran content, the LC mesophase breadth decreased by slightly increasing the glass transition temperature and decreasing the clearing temperature. This indicates the spiropyran molecule destabilizes the order necessary for the formation of a LC phase. Above 50% spiropyran content, a LC phase could not be observed by optical microscopy, DSC, or X-ray diffraction. **V** and **VI** exhibited substantially higher $T_g$'s of 80 and 140 °C, higher than those exhibited by the LC compounds **I**−**IV**. POM indicated that **I**−**IV** exhibited cholesteric phases as indicated by Grandjean oily streaks (Figure 2a), **IX** exhibited a higher temperature cholesteric phase and a lower temperature smectic-A phase as indicated by large focal-conic fans and homeotropic regions (Figure 2B), and **VIII** exhibited a nematic phase as indicated by large droplets near clearing as shown in Figure 2C. The thermal transitions and mesophase types of **VIII** and **IX** are similar to their respective homopolymers.[17]

**X-ray Diffraction.** The LC order present in these cholesteric siloxanes decreased with increasing spiropyran content as shown by X-ray diffraction. As the spiropyran content increases, the primary layer intensity, due to the repeat distance of localized clusters of molecules, becomes steadily weaker when compared to the wide angle reflection intensity. The strength of the primary layer reflection is indicative of a tendency of the LC system to layer pack. The wide angle reflection, present in all LC compounds, arises due to the side to side interactions of individual mesogens. The strongest primary reflection was exhibited by **I**, while the weakest was exhibited by **IV**. **V** exhibited no primary reflection and a weak amorphous ring at wide angles characteristic of amorphous systems. No dependence of this *d*-spacing (25 Å) was observed with mesogen composition, indicating the packing units responsible for this

**Table 2. Thermal and Optical Properties of Photochromic Siloxanes**

| siloxane | theoretical A/B/C Ratio | thermal transitions (°C) | λ max | | Dl | |
|---|---|---|---|---|---|---|
| | | | before[a] | after[a] | before[b] | after[b] |
| **I** | 0/50/50 | g 50 *n** 220 i | 523 | 523 | 83 | 83 |
| **II** | 10/45/45 | g 62 *n** 195 i | 509 | 500 | 94 | 70 |
| **III** | 15/42.5/42.5 | g 65 *n** 180 i | 507 | 483 | 102 | 64 |
| **IV** | 20/40/40 | g 65 *n** 170 i | 465 | 453 | 82 | 65 |
| **V** | 50/25/25 | g 80 viscous melt | N/A | N/A | N/A | N/A |
| **VI** | 100/0/0 | g 140 viscous melt | N/A | N/A | N/A | N/A |
| **VII** | 100/0/0 | g 70 viscous melt | N/A | N/A | N/A | N/A |
| **VIII** | 10/90/0 | k1 70 k2 110 *n* 150 i | N/A | N/A | N/A | N/A |
| **IX** | 10/0/90 | g 75 SA 205 *n** 230 i | N/A | N/A | N/A | N/A |

[a] Measured reflection band maximum before/after irradiation with UV. [b] Bandwidth defined as FWHM of reflection peak.

**Table 3. Spectral and Thermal Decoloration Kinetic Data of Photochromic Siloxanes**

| compd | λ max (nm) absorption of the colored form[a] | λ max (nm) fluorescence of the colored form[b] | thermal decay constants ($s^{-1}$)[c] |
|---|---|---|---|
| AlBIPS | 606 | | $2.8 \times 10^{-2}$ |
| PtBIPS | 606 | | $3.7 \times 10^{-2}$ |
| II | 602 | 680 | $2.2 \times 10^{-2}$ |
| III | 604 | 688 | $1.8 \times 10^{-2}$ |
| IV | 604 | 695 | $k_1$ $1.8 \times 10^{-2}$ |
| | | | $k_2$ $1.5 \times 10^{-2}$ [d] |
| V | 600 | 693 | $k_1$ $1.8 \times 10^{-2}$ |
| | | | $k_2$ $6.7 \times 10^{-3}$ [d] |
| VI | 602 | 695 | multiexponential[e] |
| VII | 598 | 696 | multiexponential[e] |
| VIII | 603 | 702 | $k_1$ $1.9 \times 10^{-2}$ |
| | | | $k_2$ $6.6 \times 10^{-3}$ [d] |
| IX | 602 | 694 | multiexponential[e] |

[a] Absorption measurements were done in toluene taken after irradiation with 365 nm. Decay kinetics was carried out at room temperature. [b] Fluorescence studies were done on sheared thin films after melting the siloxanes. [c] Thermal decay measurements were done in toluene. [d] Rate constants $k_1$ and $k_2$ were measured from fit to exponential decay; $A = a_1 \exp(-k_1 t) + a_2 \exp(-k_2 t)$. [e] Decay was more than the two-exponential type.

reflection do not change in size but slowly disappear, thus suggesting that the bulky spiropyran molecule is not conducive to efficient packing.

**Selective Reflection. I–IV** when sheared in the cholesteric phase and quenched to room temperature exhibit selective reflection bands in the visible. The reflection wavelength and bandwidth are shown in eqs 1 and 2

$$\lambda = nP \text{ reflection wavelength} \quad (1)$$

$$\Delta\lambda = \Delta nP \text{ reflection bandwidth} \quad (2)$$

$P$ refers to the pitch; $n$ is the refractive index. The selective reflection wavelengths (Table 2) decreased as the spiropyran content increased, consistent with the chiral nature of the spiropyran molecule. As the composition of chiral molecules (cholesterol and spiropyran) increases, the overall helical twisting power of the system increases causing a blue shift in the reflection wavelength maximum consistent with theory.[18] Interestingly, the reflection wavelength maximum further decreases upon UV irradiation for **II–IV**, indicating the merocyanine form increases the helical twisting power relative to a closed spiropyran. No changes were observed in the reflection spectra for compound **I** containing no spiropyran. For **II–IV**, the reflection bandwidths also shrunk, considerably, upon irradiation. No trends with composition were observed for the bandwidth before or after irradiation. In general, the bandwidth should decrease with chiral content, according to eqs 1 and 2. If the pitch changes upon irradiation, then both wavelength and bandwidth would change correspondingly. If this was the case, the ratio of the reflection wavelength to bandwidth should be equal before and after irradiation. This is not seen, implying some change in the refractive index may occur due to the spiropyran ring opening.

**Electronic Spectra and Thermal Decoloration Kinetics.** Our studies on the spiropyran-bound siloxanes show that the spectral and kinetic aspects of the photochromic behavior are influenced by the molecular association of the merocyanine forms. Table 3 gives the absorption maximum of the merocyanine form and the thermal decoloration rates of the colored form in toluene. The λ absorption maximum in the closed and open forms of the spiropyran mesogen is not strikingly affected by its attachment to the siloxane ring. This is true regardless of the concentrations of all three mesogens. The λ maximum in toluene when compared to sheared films shows that there is a small hypsochromic shift (6 nm) in sheared films. In a more polar solvent like methyltetrahydrofuran (MeTHF), a larger hypsochromic shift (14 nm) was observed, consistent with the high-dipolar character of the ground state merocyanine form. The absorption spectra in both toluene and MeTHF show a shoulder around 562 nm which is characteristic of merocyanine dimer formation during the thermal decay.[19,20] It is well known that the merocyanine of 6-nitrospiropyran has a strong tendency to aggregate.[19] Figure 3 shows the spectra of **III** in toluene during the thermal decoloration. Both the λ max (602 nm) and the shoulder (562 nm) are seen in all the spectra, and no shift in the λ max is seen. The broad shape of the spectra is due to the overlap of the dimer spectrum with a λ maximum at 560 nm and that of the monomer at 600 nm. This behavior was seen for **II–IV**, **VIII**, and **IX** and also in the unattached AlBIPS and PtBIPS. In solid films of **II–IV**, the shoulder at 562 nm was not evident. Also, no broadening in the region 450–550 nm was seen, indicating the absence of dimer formation. This is plausible as the mobility of the merocyanines in a solid film is restricted at room temperature. However at elevated temperatures (60 °C), evidence of dimer formation was seen, including a broadening of the absorption band from 500 to 650 nm. Heating causes thermal mobility of the merocyanine forms promoting aggregation, probably because the glass transition temperature is being approached.

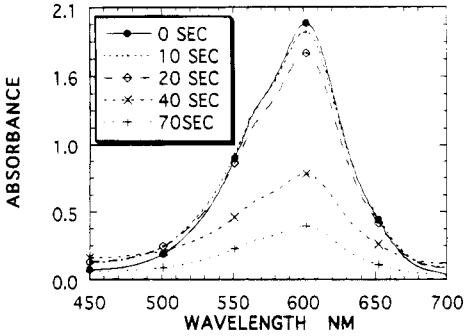


**Figure 3.** Absorption spectra of compound **III** in toluene during decoloration of the merocyanine form.

In contrast, the spectral behavior of the siloxanes containing only spiropyrans, **VI** and **VII**, are different. The absorption maximum of **VI** and **VII** (Table 3) are slightly blue-shifted in toluene compared to those of AlBIPS and PtBIPS, and a noticeable shoulder at 562 nm is also seen (Figure 4). The thermal decoloration, as seen in the spectra, showed a gradual shifting of the maximum to the blue, the maximum at 595 nm disappeared, and the peak shifted to 562 nm (Figure 4). It is likely that the thermal equilibrium is now shifted toward the dimers and, as observed earlier, the broadening of absorption in the range 460–580 nm is connected with the association of the merocyanine molecules in molecular stacks made up of very short ones, probably the dimers.[19,20] The high concentration of merocyanines and the close proximity of their distribution may favor the stabilization of such a stack in **VI** and **VII**, but in the presence of cholesterol and biphenyl, such a transformation may be sterically hindered. The sheared thin films of **VI** and **VII** when UV adapted showed a λ max

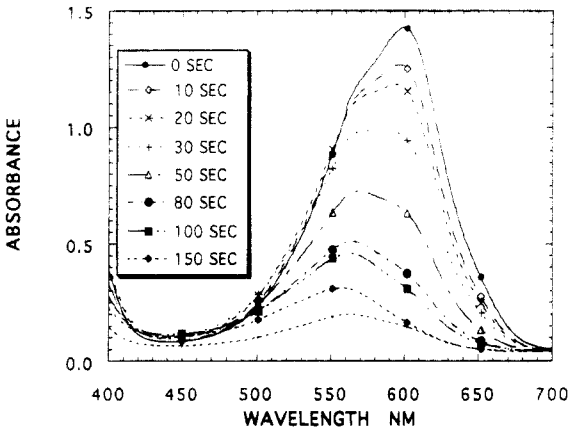


**Figure 4.** Absorption spectra of compound **VII** in toluene during decoloration of the merocyanine form.

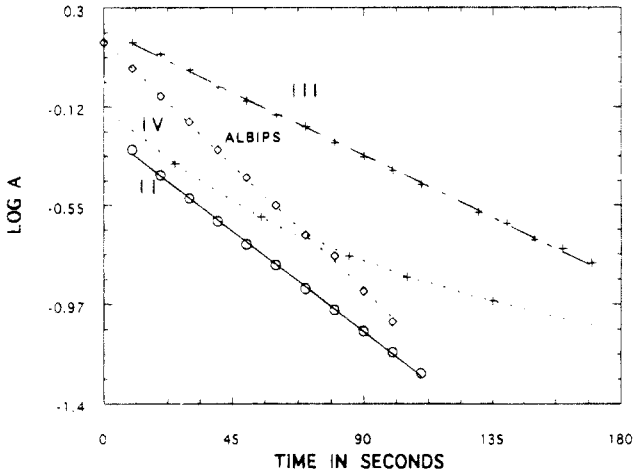


**Figure 5.** Decay curves for thermal decoloration of the siloxanes in toluene measured at 600 nm.

at 592 nm. There was some broadening of the spectrum in the 500–650 nm region, although no shoulder at 562 nm was evident. As in the case of the other siloxanes, heating the films resulted in the shift of $\lambda$ max to 562 nm, suggesting dimer formation facilitated by an increase of free volume.

The kinetics of the thermal decoloration was studied by following the decrease of absorption at the maximum (600 nm) of the colored 'merocyanine' form in toluene. Kinetics was followed up to >90% change in absorption. It is seen from Table 3 that the decay followed first-order kinetics in the unattached mesogens AlBIPS and PtBIPS and also in the siloxanes **II** and **III** (Figure 5). As expected, the decay is faster in the free mesogens. PtBIPS decays faster than ALBIPS, which may be understood in terms of increased flexibility of the carbon chain in the former. The larger flexibility of the longer spacer would permit the merocyanine groups to escape from stacks easily and thus avoid the steric hindrance for the ring closure. When attached to the siloxane ring in the presence of cholesterol and biphenyl, the decay is slower. With an increase of spiropyran content in the siloxanes (**II** and **III**), the decay rate decreases and it is no longer exponential in **IV** and **V** (Figure 5). Instead, the decay is biexponential with a fast initial decay followed by a slow long term decay. The fast initial decay is almost the same for **III**–**V** and **VIII**. The nonexponential nature of the color decay in the UV-irradiated siloxanes with increasing spiropyran concentration is indicative of the steric hindrance to the thermal merocyanine ring closure by the surrounding

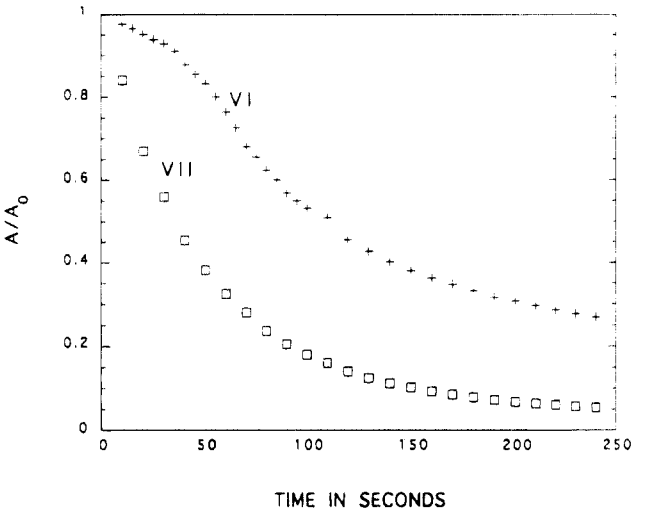


**Figure 6.** Decay curves for thermal bleaching of the siloxanes **VI** and **VII** in toluene at 600 nm.

bulky photochromic groups. Similar observation was also made for the spironaphthoxazines attached to siloxane polymers.[9] In the case of siloxanes **VI** and **VII**, the decays are both multiexponential, although differences exist (Figure 6). **VII** possessing a longer spacer exhibits a much faster initial decay, whereas **VI** with a shorter spacer shows slow initial decay followed by a faster one. Analysis shows the decays are not the two-exponential type. The larger flexibility of the five-carbon spacer in **VII** would enhance the ease of merocyanine ring closure during the decay, while in the three-carbon spacer there seems to be strong steric resistance.

Table 3 lists the fluorescence maximum of the merocyanine form of the spiropyran siloxanes measured in melted and sheared thin glassy films. The spectra were recorded by excitation at the $\lambda$ maximum of absorption. In toluene, the fluorescence could not be measured with certainty as the emission was very weak. It is known that the closed form of 6–nitro–BIPS is nonfluorescent while the merocyanine formed by irradiation does fluoresce.[21] The quantum yield of the fluorescence is very low ($10^{-2}$), due to the rapid deactivation of the excited state as a result of stereoisomerization.[21] Also, the presence of a nitro group promotes fast intersystem crossing to the triplet state. We observed that the unirradiated siloxane films were not fluorescent. The UV-irradiated films exhibited weak red emission which may be assigned to the merocyanine fluorophore. A small red shift in $\lambda$ max with increasing spiropyran content was seen for compounds **III**–**V**. The $\lambda$ max and the shape of the emission spectra did not change with varying excitation wavelengths (500–620 nm), indicating that the emission is from the monomeric merocyanines.

In conclusion, we have demonstrated how steric problems of laterally attached bulky spiropyran groups affect the synthesis, reactivity, and phase behavior of a series of cyclic siloxanes. Aggregation phenomenon and thermal decay kinetics in solution are also influenced by this lateral attachment. With increasing spiropyran content, as indicated by the change in the order of the decay kinetics, steric interactions of the bulky photochromic groups become more pronounced.

**Acknowledgment.** The authors acknowledge the constant encouragement and the facilities provided for this work by Dr. Robert L. Crane, Dr. W. W. Adams,

and Dr. T. M. Cooper of Materials Directorate, Wright Laboratory, Wright Patterson Air Force Base. Dr. L. V. Natarajan gratefully acknowledges the support of the United States Air Force through contract F33615-90-C-5911.

## References and Notes

(1) Clarson, S. J. In *Siloxane Polymers*; Clarson, S. J., Semlyen, J. A., Eds.; Prentice Hall: New York, 1992; Chapters 1 and 2.
(2) Pinsl, J.; Brauchle, C.; Kreuzer, F. H. *J. Mol. Electron.* **1987**, *3*, 9.
(3) Ortler, R.; Brauchle, C.; Miller, A.; Riepl, G. *Makromol. Chem., Rapid Commun.* **1989**, *10*, 5.
(4) (a) Tokarski, Z.; Epling, R. I.; Bunning, T. J.; McGivern; Crane, R. L. In *Organic and Biological Optoelectronics*, SPIE Proceedings; Rentzepis, P. M., Ed.; The International Society for Optical Engineering, 1993; Vol. 1853, p 60. (b) Wang, H.; Yin, M. Y.; Jarnagin, R. C.; Samulski, E. T. In *Organic and Biological Optoelectroncs*, SPIE Proceedings; Rentzepis, P. M., Ed.; The International Society for Optical Engineering, 1993; Vol. 1853, p 89.
(5) Cabrera, I.; Krongauz, V.; Ringsdorf, H. *Angew. Chem.* **1987**, *99*, 1204.
(6) Yitchaik, S.; Cabrera, I.; Buchholtz, F.; Krongauz, V. *Macromolecules* **1990**, *23*, 707.
(7) Cabrera, I.; Krongauz, V. *Macromolecules* **1987**, *20*, 2713.
(8) Krongauz, V. In *Photochromism, Molecules and Systems*; Durr, H., Bones-laurent, H., Eds.; Elsevier: Amsterdam, 1990; p 793.
(9) Yitzchaik, S.; Ratner, J.; Buchholtz, F.; Krongauz, V. *Liq. Cryst.* **1990**, *8*, 677.
(10) Zelichenok, A.; Buchholtz, F.; Yitzchaik, S.; Ratner, J.; Safro, M.; Krongauz, V. *Macromolecules* **1992**, *25*, 3179.
(11) Natarajan, L. V.; Bunning, T. J.; Klei, H. E.; Crane, R. L.; Adams, W. W. *Macromolecules* **1991**, *24*, 6554.
(12) Natarajan, L. V.; Bunning, T. J.; Tondiglia, V.; Patnaik, S.; Pachter, R.; Crane, R. L.; Adams, W. W. In *Chemistry of functional dyes*; Shirota, Y., Ed.; Mita Press: Kobe, 1993; Vol. 2, p 405.
(13) Natarajan, L. V.; Tondiglia, V.; Bunning, T. J.; Crane, R. L.; Adams, W. W. *Adv. Mater. Opt. Electron.* **1992**, *1*, 293.
(14) Hassner, A.; Alexian, V. *Tetrahedron Lett.* **1978**, *46*, 4475.
(15) Drew, D.; Doyle, J. R. In *Inorganic Synthesis*; Cotton, F. A., Ed.; McGraw Hill: New York, 1971; Vol. XIII, p 47.
(16) Kreuzer, S. H.; Andrejewski, D.; Haas; Habele, W.; Riepel, G.; Spes, R. *Mol. Cryst. Liq. Cryst.* **1991**, *199*, 345.
(17) Bunning, T. J.; Klei, H. E.; Samulski, E. T.; Adams, W. W.; Crane, R. L. *Mol. Cryst. Liq. Cryst.* **1993**, *231*, 163.
(18) Jacobs, S. D. In *Handbook of Laser Science and Technology*; Weber, M. J., Ed.; CRC Press: Boca Raton, FL, 1986; Vol. 4, Part 2, p 409.
(19) Goldburt, E.; Shvartsman, K.; Fishman, S.; Krongauz, V. *Macromolecules* **1984**, *17*, 1225.
(20) Eckhardtl, H.; Bose, A.; Krongauz, A. *Polymer* **1987**, *28*, 1959.
(21) Bertelson, R. C. In *Photochromism*; Brown, G. H., Ed.; Wiley-Interscience, New York, 1971; p 201.